Online Appendix

Supplementary Methods

RNA isolation. Mice were killed by cervical dislocation and tissues (epididymal fat, liver, and skeletal muscle) were collected, snap frozen in N_2, and stored at -80 °C. Total RNA was extracted and purified using RNeasy (Qiagen, Chatsworth, CA).

cRNA preparation, array hybridization, and comparative microarray analysis. Microarray analysis was performed as previously described (1). RNA pooled from two to three mice was used for cRNA synthesis. cRNA was hybridized on Affymetrix (Santa Clara, CA) murine chips U74Av.2. Two to five chips were used for each experimental condition. All microarray data is available at the Diabetes Genome Anatomy Project (DGAP) website (http://www.diabetesgenome.org).

Comparative microarray analysis. The robust multi-array average algorithm (2) was first applied to normalize and scale the probe set intensities across all microarrays. Subsequently, the Linear Models for Microarray Data package (3) was employed to assess the differential expression of each probe set between B6 and 129 samples. For each probe set, the relative fold-change and the significance value of the differential expression (*P*-value) were retained for further analysis. Probe sets were converted to genes based on the mapping provided by Affymetrix. In cases where multiple probe sets mapped to the same gene, the probe set showing the greatest variance was selected. Finally, the mouse genes were mapped onto their human homologs through NCBI Homologene Version 63. When multiple human homologs exist for the same mouse gene, each human homolog was annotated with the expression value of the mouse gene. When multiple mouse genes mapped to the same human one, only the mouse gene with the most significant *P*-value between B6 and 129 samples was used.

Integrating gene expression data onto a protein-protein interaction network. A protein-protein interaction network was compiled from the Human Protein Reference Database Version 7 (4). All protein-protein interactions from the database were used, excepting those with only yeast-2-hybrid experimental evidence. Nodes (proteins) in the network were annotated by the z-score of the *P*-value of the corresponding gene in B6 vs. 129 mice. Nodes missing *P*-values (because of absent genes on the microarray), along with all interactions involving them, were removed from the final network. In total, 4959 genes were retained for further analysis.

Gene Network Enrichment Analysis. The Active Modules algorithm (5) was applied to the integrated network to identify subnetworks with a strong cumulative significance value in B6 vs. 129 mice. In particular, subnetworks were identified by optimizing for a subnetwork score defined as the standard Stouffer's z-score (6) using simulated annealing. The algorithm was applied to the dataset 100 times and all subnetworks from the different applications were retained. The hypothesis here is that each subnetwork represents a different approximation of the true, differentially active gene network in B6 vs. 129 mice. If so, a more robust estimate of the true network can be generated by taking the consensus between the different approximations rather than any particular one. This concept of averaging stochastically computed predictors (a type of ensemble learning) – is routinely done in machine learning to reduce errors stemming from the variances or biases of individual predictors. Some examples include commonly used decision tree learning systems, such as Random Forests (7).

Individual gene *P*-values were calculated from the network analysis as follows: For each gene *g,* the number of times it appears in the identified subnetworks was tallied and denoted as

O_g. The class labels of the gene expression profiles were then permuted and the entire pipeline — the comparative microarray analysis to calculate p-values, multiple applications of Active Modules to find sub-networks, and tallying of genes in the identified sub-networks — were repeated under each permutation. This generated a background distribution for each gene *g* and a *P*-value could then be estimated by comparing the O_g against the gene-specific background. The *P*-values were subsequently converted to z-scores under a standard normal distribution and referred to as Membership in Active Networks scores (MAN-scores). Multiple hypotheses correction (Benjamini-Hochberg) was then applied to control the false detection rate across all genes. Genes with FDR $\leq$ 0.25 were considered significant. These MAN-score *P*-values represent the relative probability of each gene to belong to the true differentially active network as estimated by the algorithm.

Biological processes from the Gene Ontology Consortium (8) and the Molecular Signatures Database (9) were tested for over-representation of high MAN-scoring genes. Namely, for each gene set, the Mann-Whitney U statistic was calculated from ordering genes by their MAN-scores. A *P*-value could be determined by comparing the U statistic against a background distribution of U statistics estimated from 1000 randomly chosen gene sets of the same size. The *P*-values were corrected for multiple hypotheses testing using the method of Benjamini-Hochberg (10).

To visualize biological process networks, the genes in each biological process, together with all statistically significant interacting neighbors (network analysis FDR $\leq$ 0.25) were selected from the protein-protein interaction network along with all of their common edges.

It is important to emphasize that the detection of sub-networks predicted to be differentially active is independent of the later step of enrichment testing. Sub-networks are detected on the basis of their mean z-score and general connectivity (5), without consideration of functional annotation. Conversely, while the enrichment testing of affected signaling pathways clearly does depend on functional annotation, the gene networks associated with the statistically significant pathways (from the last step of the algorithm) include genes that are not annotated as part of each pathway but nonetheless interact with pathway members. Together, these two features mean that mistaken, missing, or overlapping functional annotations of genes (11) only partially affect the composition of the process specific sub-networks the algorithm produces. Therefore, the algorithm is actually less sensitive to errors of annotation than other common enrichment approaches (9,12).

Quantitative RT-PCR. cDNA was prepared from 1 μg of RNA by using High Capacity cDNA Reverse Transcription Kit (Applied Biosystems, Foster City, CA). 0.25 μL of cDNA was used in a 10 μL PCR (Maxima SYBR Green qPCR Master Mix; Fermentas, Glen Burnie, MD) containing 250 nM of each specific primer. Reactions were run in duplicate using the ABI Prism 7900 Sequence Detection System (Applied Biosystems, Foster City, CA) under the following conditions: 50 ºC-2 min, 95 ºC-10 min, and 40 cycles of 95 ºC-15s, 60 ºC-20s, and 72 ºC-30s. Dissociation protocols were conducted after every run to check for primer specificity. To obtain relative expression values, we calculated the $2^{-\Delta Ct}$ parameter for each individual sample using the TATA binding protein (TBP) mRNA Ct value as a reference. Primer sequences are given in Supplementary Table S4.

Stromalvascular fraction isolation. Mice were killed and the epididymal adipose tissue was removed, minced, and digested with 1 mg/ml collagenase, type 1 (Worthington, Lakewood, NJ) for 30 min at 37°C under constant agitation in Dulbecco's Modified Eagle Medium (DMEM) containing 1% bovine serum albumin (Sigma-Aldrich, St. Louis, MO). After digestion, tissues

were filtered through 150-mm nylon mesh and centrifuged at 500 × g for 5 min. The supernatant containing isolated adipocytes was removed and the pellet, representing the stromalvascular fraction, was re-suspended and washed twice with PBS, 2% fetal bovine serum (FBS). Erythrocytes were depleted from the stromalvascular fraction by incubating the pellet of cells with ACK lysis buffer (Lonza; Basel, Switzerland) for 5 min at 4°C. Cells were then centrifuged at 500 × g for 5 min and washed once with PBS, 2% FBS.

Flow cytometry. Erythrocyte-free stromal vascular fraction cells were incubated in PBS, 2% FBS containing 5 μg/mL of anti-CD16/CD32 for 10 min at 4°C to block non-specific staining. The mix of antibodies against different surface markers was added to the cells and incubated for additional 10 min at 4°C. Cells were washed once with PBS, 2% FBS and analyzed using the LSRII flow cytometer (BD Biosciences, San Jose, CA). When using biotin labeled antibodies, an additional incubation with 10 μg/mL Streptavidin, Alexa Fluor® 610-PE for 25 min at 4°C was included in the protocol. To test for cell viability, 0.1 mg/ml of propidium iodide (Sigma-Aldrich; St. Louis, MO) was added to the cells 1-2 minutes prior the analysis. Antibodies anti-CD45, PE-Cy7; CD11c, PE; F4/80, biotin; and Ter-119, APC were purchased from Ebioscience (San Diego, CA). Anti-CD11b, APC-Cy7; and anti-CD4, PE were obtained from BD Biosciences (San Jose, CA). Anti-CD3, Pacific Blue was purchased from BioLegend (San Diego, CA). Working concentration of antibodies varied from 0.5 μg/mL (anti-CD11b) to 5 μg/mL (anti-F4/80), although the majority of the antibodies were used within the concentration range of 1-2 μg/mL.

Reference List

1. Almind,K, Kahn,CR: Genetic determinants of energy expenditure and insulin resistance in diet-induced obesity in mice. *Diabetes* 53:3274-3285, 2004
2. Irizarry,RA, Hobbs,B, Collin,F, Beazer-Barclay,YD, Antonellis,KJ, Scherf,U, Speed,TP: Exploration, normalization, and summaries of high density oligonucleotide array probe level data. *Biostatistics* 4:249-264, 2003
3. Smyth,GK: Linear models and empirical bayes methods for assessing differential expression in microarray experiments. *Stat Appl Genet Mol Biol* 3:Article3, 2004
4. Keshava Prasad,TS, Goel,R, Kandasamy,K, Keerthikumar,S, Kumar,S, Mathivanan,S, Telikicherla,D, Raju,R, Shafreen,B, Venugopal,A, Balakrishnan,L, Marimuthu,A, Banerjee,S, Somanathan,DS, Sebastian,A, Rani,S, Ray,S, Harrys Kishore,CJ, Kanth,S, Ahmed,M, Kashyap,MK, Mohmood,R, Ramachandra,YL, Krishna,V, Rahiman,BA, Mohan,S, Ranganathan,P, Ramabadran,S, Chaerkady,R, Pandey,A: Human Protein Reference Database--2009 update. *Nucleic Acids Res* 37:D767-D772, 2009
5. Ideker,T, Ozier,O, Schwikowski,B, Siegel,AF: Discovering regulatory and signalling circuits in molecular interaction networks. *Bioinformatics* 18 Suppl 1:S233-S240, 2002
6. Folks,JL: Combination of independent tests. In *Handbook of statistics: Nonparametric methods*. Sen,PK, Krishnaiah, PR, Eds. Amsterdam, Elsevier, 1984, p. 113-121
7. Breiman,L: Random Forests. *Machine Learning* 45 (1):5-32, 2001
8. Ashburner,M, Ball,CA, Blake,JA, Botstein,D, Butler,H, Cherry,JM, Davis,AP, Dolinski,K, Dwight,SS, Eppig,JT, Harris,MA, Hill,DP, Issel-Tarver,L, Kasarskis,A, Lewis,S, Matese,JC, Richardson,JE, Ringwald,M, Rubin,GM, Sherlock,G: Gene ontology: tool for the unification of biology. The Gene Ontology Consortium. *Nat Genet* 25:25-29, 2000

9. Subramanian,A, Tamayo,P, Mootha,VK, Mukherjee,S, Ebert,BL, Gillette,MA, Paulovich,A, Pomeroy,SL, Golub,TR, Lander,ES, Mesirov,JP: Gene set enrichment analysis: a knowledge-based approach for interpreting genome-wide expression profiles. *Proc Natl Acad Sci U S A* 102:15545-15550, 2005

10. Benjamini,Y, Hochberg,Y: Controlling the false discovery rate: a practical and powerful approach to multiple testing. *Journal of the Royal Statistical Society, Series B (Methodological)* 57 (1):289-300, 1995

11. Murali,TM, Wu,CJ, Kasif,S: The art of gene function prediction. *Nat Biotech* 24(12):1474-1475, 2006

12. Huang,DW, Sherman,BT, Lempicki,RA: Systematic and integrative analysis of large gene lists using DAVID Bioinformatics Resources. *Nature Protoc* 4(1):44-57, 2009

Supplementary Figure S1. Histology of epididymal adipose tissue of B6 and 129 mice. (A) Samples were stained with hematoxylin/eosin and documented using digital camera coupled with optical microscopy at the magnitude of 200x. The arrow indicates crown-like structures. Panels are representative of 5 different animals per group. (B) The area of at least 50 adipocytes per animal was quantified and mean ± SEM was represented. *** $P < 0.001$ vs. 129.

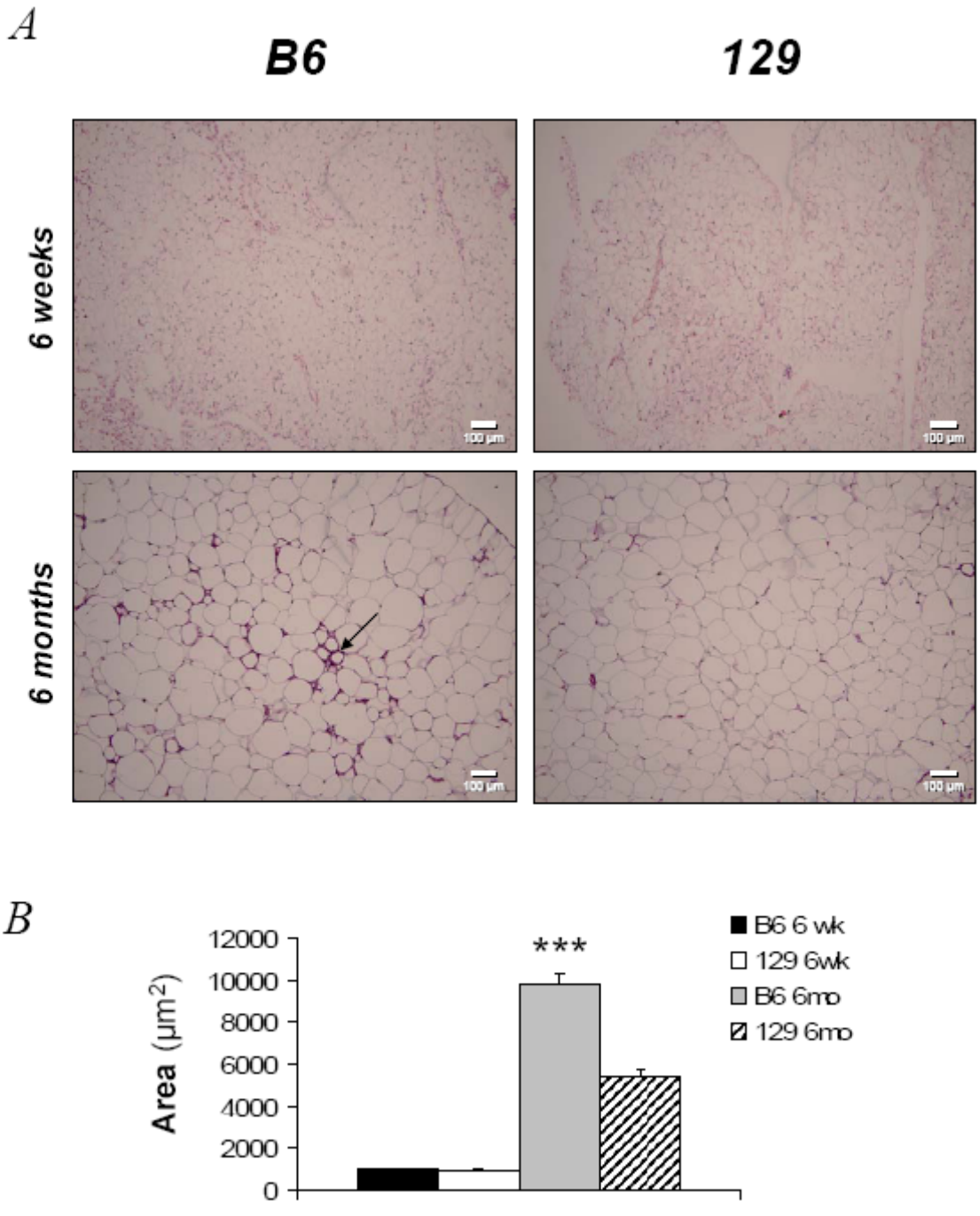

Supplementary Figure S2. Network view of the immune system process differences in adipose tissue of B6 and 129 mice at 6 weeks (left) and 6 months (right) of age. The gene network was generated by mapping genes that were significantly over-represented in B6 vs. 129 mice (*Q-value* < 0.25) among the Gene Network Enrichment Analysis results at 6 months intersected with those at 6 weeks onto protein-protein interaction networks involving genes annotated with the IMMUNE SYSTEM PROCESS gene set. Red genes are higher than 2-fold in 129 compared to B6; green ones are higher than 2-fold in B6 compared to 129. Genes are denoted by an upward or downward triangle if the fold-change at 6 months is greater or smaller than that at 6 weeks, respectively, and the size denotes the magnitude of the difference. Arrows represent genes with specific interest commented on the main text.

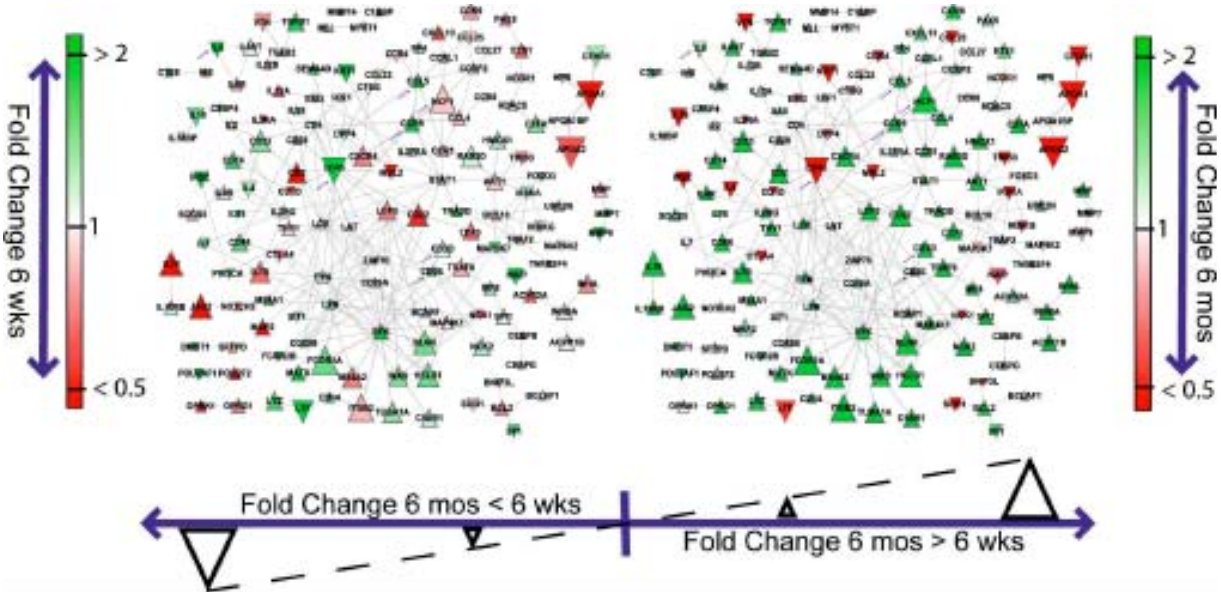

Supplementary Figure S3. Gene networks associated with inflammatory markers in adipose tissue of B6 and 129 mice at 6 weeks (left) and 6 months (right) of age. Gene networks were generated by mapping genes that were significantly over-represented in B6 vs. 129 mice (*Q-value* < 0.25) among the Gene Network Enrichment Analysis results at 6 months intersected with those at 6 weeks onto protein-protein interaction networks involving at least one interactor to each inflammatory marker: (A) CD11c, (B) CD11b, and (C) TNF. Colors range from bright red to green, corresponding to 2-fold less and 2-fold greater differences in expression between B6 and 129 at each age, respectively. Nodes point upwards if the fold change difference between B6 and 129 is greater at 6 months than at 6 weeks and downwards otherwise. The node size corresponds to the magnitude of that fold change difference between the two ages. The inflammatory network around each biomarker is drawn to scale between the two ages. Networks around different biomarkers are not to scale with each other.

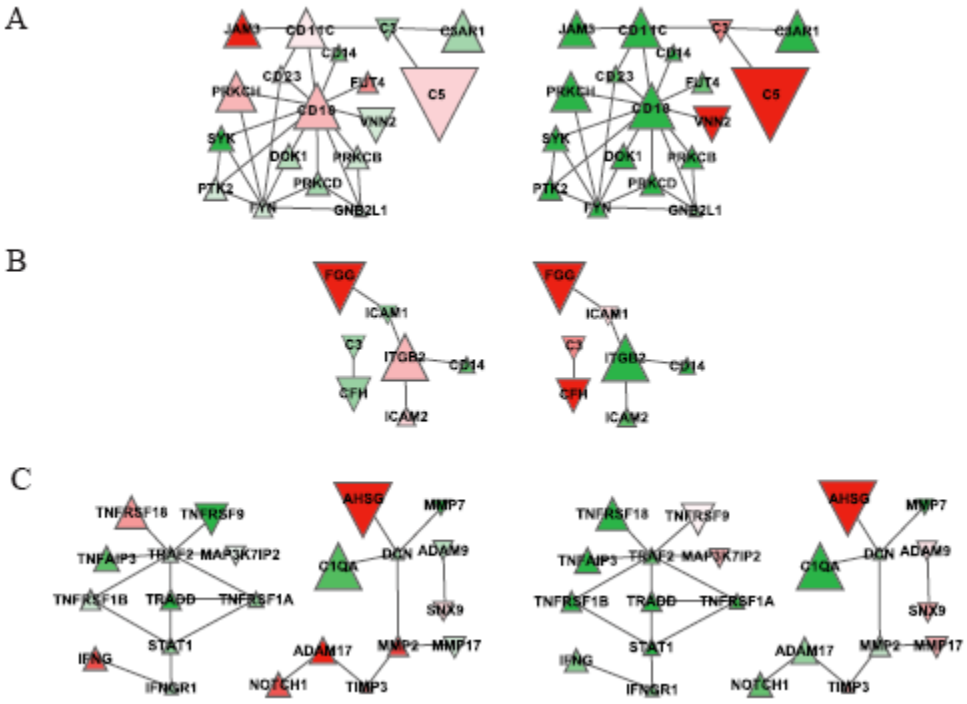

Supplementary Figure S4. Expression of inflammatory markers in (A) liver, (B) skeletal muscle, and (C) spleen of 6-week (6 wk) or 6-month (6 mo) old B6 and 129 mice. mRNA expression was assessed by qPCR. All values are normalized by TBP and expressed as fold change of the 6 weeks old B6 average value. Results represent mean ± SEM of 5-7 animals. * P < 0.05; ** P < 0.01; *** P < 0.001 vs. 129. # P < 0.05; ## P < 0.01; ### P < 0.001 vs. 6 wk.

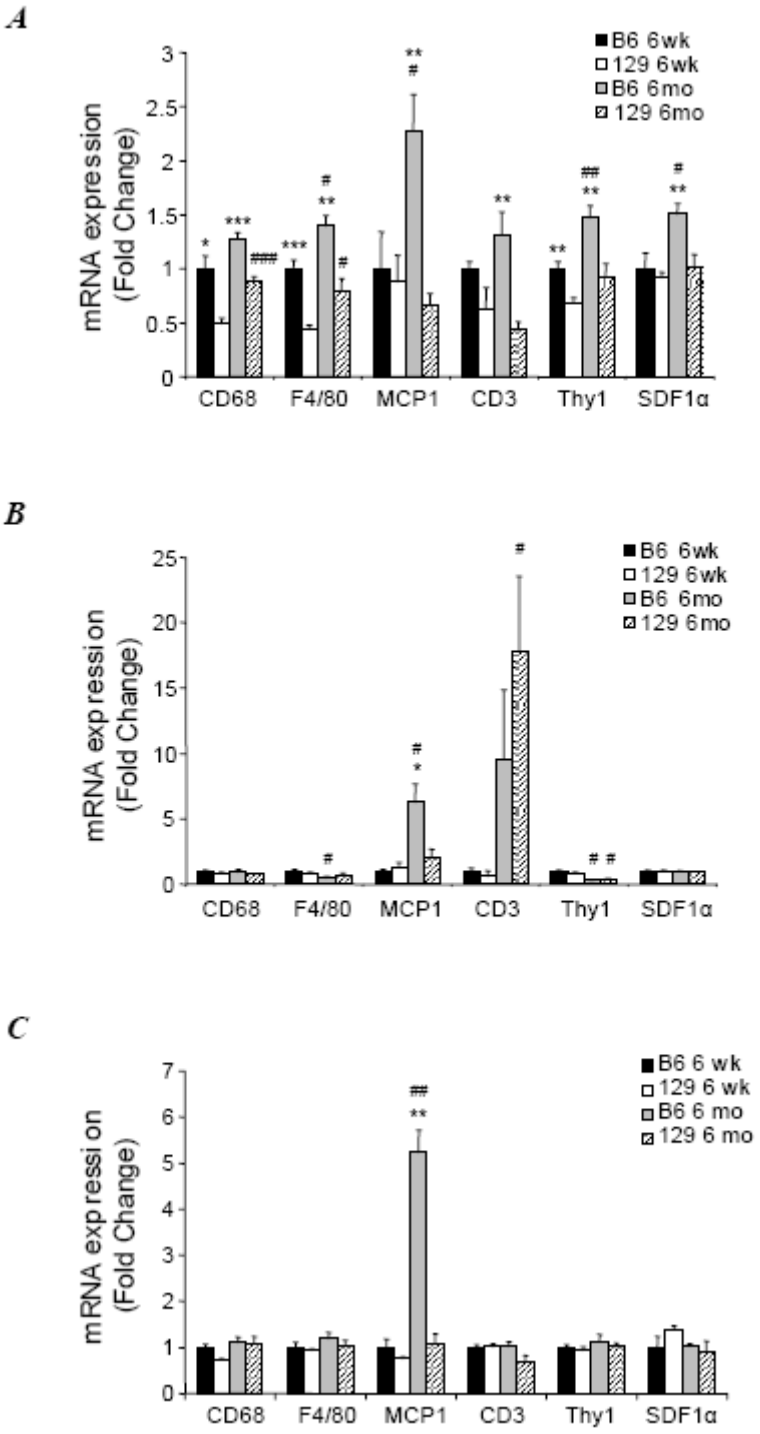

Supplementary Figure S5. Expression of inflammatory markers in epididymal adipose tissue of caloric restricted (CR) B6 mice. mRNA expression was assessed by qPCR. All values are normalized by TBP and expressed as fold change of the average values of B6 mice with *ad libitum* (ad lib) access to food. Results represent mean ± SEM of 5 animals. * $P < 0.05$; ** $P < 0.01$ vs. 6 Ad Lib.

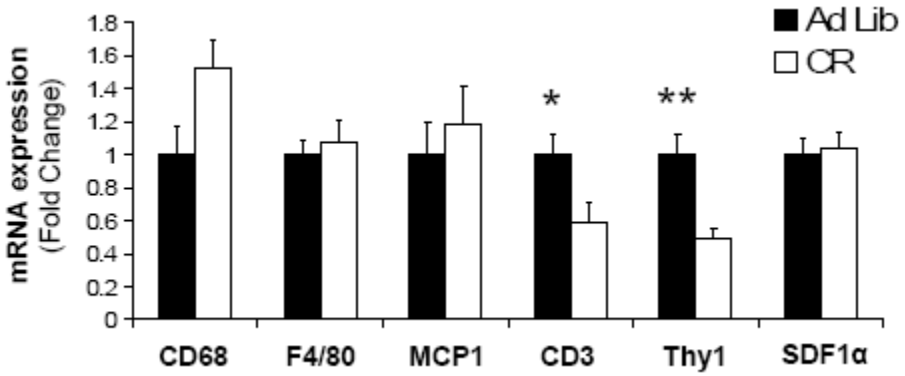

Supplementary Table S1. The top ten most significantly perturbed biological processes in adipose tissue of B6 vs. 129 mice at 6 months of age in comparison to 6 weeks of age, as revealed by GNEA.

	6 months		6 weeks	
Gene set	***P* value**	***Q* value**	***P* value**	***Q* value**
IMMUNE_SYSTEM_PROCESS	0.00001	0.00825	0.00423	0.31725
LEUKOCYTE_CHEMOTAXIS	0.00015	0.06188	0.18735	0.78859
CYTOKINE_SECRETION	0.00024	0.06600	0.02777	0.49804
PROTEOLYSIS	0.00035	0.07219	0.03395	0.49804
REGULATION_OF_CYTOKINE_SECRETION	0.00056	0.09075	0.00474	0.32588
IMMUNE_RESPONSE	0.00071	0.09075	0.06614	0.64476
LEUKOCYTE_MIGRATION	0.00077	0.09075	0.27520	0.81376
CELL_SUBSTRATE_ADHESION	0.00124	0.12788	0.30998	0.82188
CHEMICAL_HOMEOSTASIS	0.00213	0.19525	0.49443	0.90836
MITOTIC_SPINDLE_ORGANIZATION_AND_BIOGENESIS	0.00304	0.23227	0.33681	0.84081

Supplementary Table S2. The most significantly perturbed biological processes in the adipose tissue of B6 versus 129 mice at 6 weeks of age as revealed by Differential Expression Analysis, Gene Set Enrichment Analysis, and Gene Network Enrichment Analysis.

Gene Set Enrichment Analysis, 6 weeks			
Geneset	Size	P.Value	FDR
REGULATION_OF_G_PROTEIN_COUPLED_RECEPTOR_PROTEIN_SIGNALING_PATHWAY	15	0.00000	0.04400
HUMORAL_IMMUNE_RESPONSE	26	0.00000	0.04400
CELLULAR_PROTEIN_COMPLEX_ASSEMBLY	20	0.00000	0.41425

Gene Network Enrichment Analysis, 6 weeks			
Name	Size	P.Value	FDR
AGING	13	0.00279	0.23348
BONE_REMODELING	29	0.00056	0.23348
CYTOKINESIS	19	0.00220	0.23348
GLUCOSE_CATABOLIC_PROCESS	11	0.00221	0.23348
NEGATIVE_REGULATION_OF_MULTICELLULAR_ORGANISMAL_PROCESS	32	0.00281	0.23348
NEGATIVE_REGULATION_OF_SECRETION	13	0.00161	0.23348
POSITIVE_REGULATION_OF_SIGNAL_TRANSDUCTION	123	0.00283	0.23348
REGULATION_OF_PROTEIN_SECRETION	22	0.00132	0.23348
REGULATION_OF_SIGNAL_TRANSDUCTION	217	0.00123	0.23348
TISSUE_REMODELING	30	0.00108	0.23348
IMMUNE_SYSTEM_PROCESS	329	0.00423	0.31725

Supplementary Table S3. The most significantly perturbed biological processes in the adipose tissue of B6 versus 129 mice at 6 months of age as revealed by Differential Expression Analysis, Gene Set Enrichment Analysis, and Gene Network Enrichment Analysis.

Differential Expression Analysis, 6 months			
Geneset	Size	P.Value	FDR
CYTOSKELETON_ORGANIZATION_AND_BIOGENESIS	124	0.00103	0.42410

Gene Set Enrichment Analysis, 6 months			
Geneset	Size	P.Value	FDR
RESPONSE_TO_XENOBIOTIC_STIMULUS	6	0.00000	0.00000
XENOBIOTIC_METABOLIC_PROCESS	5	0.00000	0.00082
AEROBIC_RESPIRATION	12	0.00000	0.00134
COFACTOR_BIOSYNTHETIC_PROCESS	16	0.00000	0.09723
PEROXISOME_ORGANIZATION_AND_BIOGENESIS	10	0.00000	0.11205
COFACTOR_CATABOLIC_PROCESS	8	0.00746	0.14972
COENZYME_BIOSYNTHETIC_PROCESS	7	0.04545	0.16289

Gene Network Enrichment Analysis, 6 months			
Name	Size	P.Value	FDR
IMMUNE_SYSTEM_PROCESS	329	0.00001	0.00825
LEUKOCYTE_CHEMOTAXIS9	13	0.00015	0.06188
CYTOKINE_SECRETION	18	0.00024	0.06600
PROTEOLYSIS	190	0.00035	0.07219
IMMUNE_RESPONSE	233	0.00071	0.09075
LEUKOCYTE_MIGRATION	16	0.00077	0.09075
REGULATION_OF_CYTOKINE_SECRETION	16	0.00056	0.09075
CELL_SUBSTRATE_ADHESION	39	0.00124	0.12788
CHEMICAL_HOMEOSTASISa	150	0.00213	0.19525
CELL_MATRIX_ADHESION¡	38	0.00342	0.23227
GLUCOSE_METABOLIC_PROCESS	28	0.00366	0.23227
MITOTIC_SPINDLE_ORGANIZATION_AND_BIOGENESIS	10	0.00304	0.23227
NEGATIVE_REGULATION_OF_SECRETION	13	0.00331	0.23227
APOPTOTIC_PROGRAM	60	0.00601	0.24033
CARBOHYDRATE_CATABOLIC_PROCESS	24	0.00670	0.24033
CELL_DIVISION	21	0.00448	0.24033
CELLULAR_CARBOHYDRATE_CATABOLIC_PROCESS	23	0.00670	0.24033
CYTOKINESIS	19	0.00491	0.24033
GLYCEROPHOSPHOLIPID_BIOSYNTHETIC_PROCESS	30	0.00653	0.24033
ION_HOMEOSTASIS	124	0.00514	0.24033
LOCOMOTORY_BEHAVIOR	96	0.00555	0.24033
PHOSPHOLIPID_BIOSYNTHETIC_PROCESS	39	0.00653	0.24033
RESPONSE_TO_HYPOXIA	28	0.00501	0.24033
DEFENSE_RESPONSE	267	0.00719	0.24716
AROMATIC_COMPOUND_METABOLIC_PROCESS	26	0.00769	0.25377

Supplementary Table S4. Oligonucleotides used for Sybr-Green RT-qPCRs.

Gene	Forward (5'-3')	Reverse (5'-3')
CD45	GGGTTGTTCTGTGCCTTGTT	GGATAGATGCTGGCGATGA
CCR5	ATCCGTTCCCCCTACAAGAG	GAGTAGAGTGGGGGCAGGAG
CD68	GCAGCACAGTGGACATTCAT	TTGCATTTCCACAGCAGAAG
F4/80	TTTCCTCGCCTGCTTCTTC	CCCCGTCTCTGTATTCAACC
CD11b	GAGCACCTCGGTATCAGCAT	TCCATGTCCACAGAGCAAAG
CD11c	CAGAACTTCCCAACTGCACA	TCTCTGAAGCTGGCTCATCA
CD18	CTGACCCACCTGACTGACCT	CCGTTGTCGTAGCACTCTTG
CD3	ATATCTCATTGCGGGACAGG	CCCTGAGTCCTGCTGAGTTC
Thy1	AACTCTTGGCACCATGAACC	GTTATTCTCATGGCGGCAGT
CD72	GAGAGAGCGAAGACCAAGGA	TGGCTCTCCTCCAGACTTCC
CD80	TTGGTTGGAAAATGGAAGAGA	GGGTCTTCTGGGGGTTTTT
TNF	CCACCACGCTCTTCTGTCTA	GATCTGAGTGTGAGGGTCTGG
IL6	GTTCTCTGGGAAATCGTGGA	CCAGTTTGGTAGCATCCATCA
IFNγ	GAACTGGCAAAAGGATGGTG	GCTGATGGCCTGATTGTCTT
MIF	CCCAGAACCGCAACTACAG	GACTCAAGCGAAGGTGGAAC
MCP1	AGGTCCCTGTCATGCTTCTG	TCATTGGGATCATCTTGCTG
CCL5	CTGCTGCTTTGCCTACCTCT	ACACACTTGGCGGTTCCTT
SDF1α	GCTCTGCATCAGTGACGGTA	AGATGCTTGACGTTGGCTCT
LBP	GGACTTCAGCGGGGACTT	CGATGGAAGAGTCAGAGATGG
Ly86	CTCTGATGGCAAAAGGCTCT	CCCTGTGGAACATCAAGTCC